The Controller Design of Quasi-Z-Source Inverter for PV-Rooftop System using Fuzzy controller

Patumporn Wongyai[1], **Jakkrit Pakdeeto**[2], **Koson Chaicharoenaudomrung**[3], **Kongpol Areerak**[1], and **Kongpan Areerak**[1†], Non-members

ABSTRACT

This paper presents the controller design for PV-rooftop system. This system can operate both standalone and grid connection modes. The quasi-Z-source inverter is chosen to convert the electrical power from direct current to alternating current. Both conventional PI and proposed fuzzy controllers are designed for the considered system operating in both standalone and grid connection modes. The simulation results by using the SimPowerSystem® in MATLAB and the hardware-in-loop simulation were used to confirm the effectiveness of the proposed controller. The results can confirm that the proposed fuzzy controller can provide the better performance compared with the conventional PI controller.

Keywords: Controller Design, Quasi-Z-Source Inverter, Fuzzy Logic controller, PV-Rooftop System

1. INTRODUCTION

Today, the global warming issue caused by greenhouse gases affects to increase renewable energy usage. The popular choice of renewable energy is the photovoltaic (PV) system which can operate in both standalone and grid-connected modes [1]-[2]. However, the output power of the PV system is the direct current (DC). This reason affects that the PV system cannot connect to the appliances or utility grid directly. Hence, the inverters is then required to convert the electrical power from DC to AC. Many types of single-phase inverter can convert the DC to alternating current (AC) such as half bridge inverter, full bridge inverter, class-D inverter, etc. Nevertheless, the power condition of PV system including the inverter needs to meet the requirement of high step-up voltage as similar as the buck-boost converter in the DC power system. Generally, the inverters require the high input voltage obtained from the photovoltaic in series arrays. One type of the inverters reported in [3]-[6] is the quasi-Z-source inverter (qZSI). It can be used to perform the lower input voltage requirement and it can supply the output voltage as similar as the other inverters. The qZSI was designed by F. Z. Peng in 2003 in which this inverter absorbs a continuous constant dc current from the source while the conventional ZSI draws a discontinuous current. Thus, the qZSI is suitable for the PV power system and it was reported with the better performance for the PV rooftop system. The output power from PV rooftop system will depend on the environmental conditions as follows: irradiance intensity and temperature. This reason results in the output voltage of PV system does not constant. Thus, the maximum power point tracking (MPPT) is very important to obtain the maximum power point (MPP) at any irradiance intensity. To regulate the output voltage and track the MPP for the PV rooftop system, the controller design is very important.

The qZSI can divide in two stages operation, shoot-through and non-shoot-through states, where it can be used to perform the dynamical model. In this paper, the proposed model is used for the conventional PI controller design by using the basic control theory. However, the response from the conventional controller cannot provide a good performance. To improve the better performance, the fuzzy controller is selected to apply in the considered system. The proposed fuzzy controller is designed based on both the standalone and grid-connection modes. The system responses controlled by the proposed fuzzy controller will be compared with the conventional PI controller. In addition, this paper presents the hardware-in-loop simulation to provide the results which can confirm the ability for the implementation. The results show that the proposed controller can be used to regulate the PV rooftop system in both standalone and grid connection modes. Moreover, the proposed fuzzy controller can provide the better performance compared with the PI controller.

This paper is structured in six sections as follows: the first section is an introduction, and the considered system will be described in section II. In section III, the proposed controller design is addressed. The simulation and hardware-in-loop (HIL) results are reported in part IV and V, respectively. Finally, part VI is the conclusion of this paper.

Manuscript received on January 1, 2023; revised on March 7, 2023; accepted on March 26, 2023. This paper was recommended by Associate Editor Vuttipon Tarateeraseth.

[1]The authors are with School of Electrical Engineering, Instituted of Engineering, Suranaree University of Technology, Thailand.

[2]The author is with Department of Teacher Training in Electrical Engineering, Faculty of Technical Education, KMUTNB, Thailand.

[3]The author is with Department of Electrical Engineering Technology, College of Industrial Technology, KMUTNB, Thailand.

[†]Corresponding author: kongpan@sut.ac.th

Digital Object Identifier: 10.37936/ecti-eec.2023213.251459

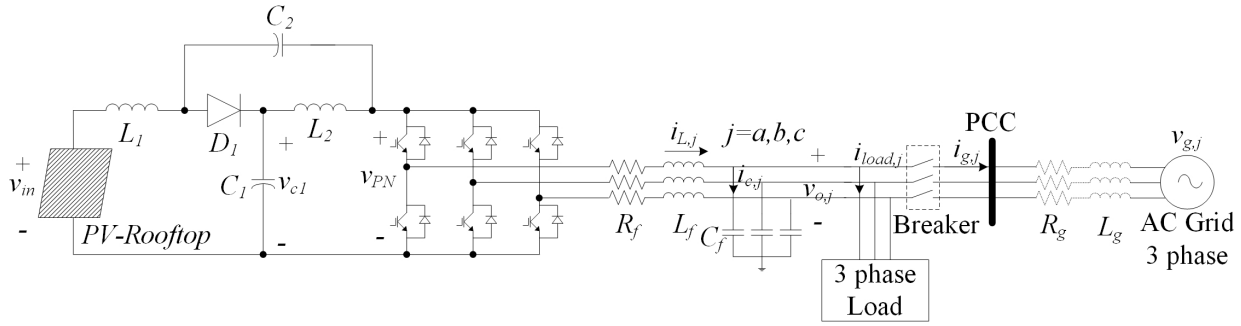

***Fig. 1**: Considered system.*

2. CONSIDERED SYSTEM

The PV rooftop system connected with the utility grid is depicted in Fig. 1, It consists of PV arrays, qZSI, filter circuit, three-phase active load, and AC utility grid.

The proposed system can be operated in two modes. The first mode is the standalone operation in which the PV rooftop is not connected with the utility grid. In this mode, the power from PV rooftop system will be only supplied to three-phase load via the qZSI.

Another mode is the grid-connected operation. The three-phase load can obtain the power from both rooftop system and utility grid. However, if the power output from PV arrays is more than the load consumption, the remaining power will be fed into the utility grid for sales with the Electricity Authority.

In contrast, if the power output from PV array is not sufficient, the three-phase load can be also received the power from the utility grid. The operational states and control modes of qZSI are explained as follows:

2.1 Operational states of qZSI network

There are two states of qZSI. The first state is the shoot-through mode occurring when the inverter's switches are short circuit and diode (*D*) is reverse bias (open circuit) as shown in Fig. 2(a). Although the voltage across the inverter is equal to 0 V ($v_{pn} = 0$ V) in this case, the current from PV arrays can be also supplied to the inverter [7]-[10]. Another state is the non-shoot-through state in which it is the normal operation and diode is forward bias (short circuit) as depicted in Fig. 2(b). Both states can be operated in order to supply the current toward the inverter continuously, resulting in uninterrupted load current operation.

From Fig. 2: the mathematical model of the considered system can be derived from the equivalent circuit in both shoot-through and non-shoot-through states. The variables are defined as follows: $L = L_1 = L_2$ and $C = C_1 = C_2$. The period time of shoot-through and non-shoot-through scenarios are set as T_0 and T_1, respectively. In addition, the switching period (T_s) can be calculated by $T_s = T_0 + T_1$ and the shoot-through duty cycle (d) is equal to T_0/T_1. After the variables are set as the previous explanations and the basic circuit theory is

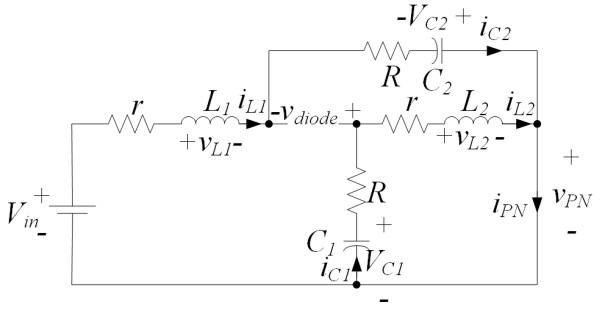

(a) shoot-through state

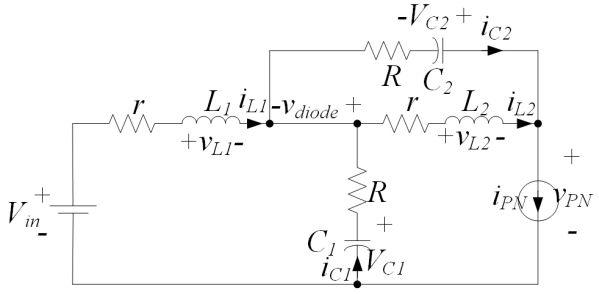

(b) non-shoot-through state

***Fig. 2**: Operational states of quasi-Z source network.*

applied, the dynamical model of the considered system can be shown in Eq. (1).

$$F\hat{\dot{x}} = \begin{bmatrix} -(R+r) & 0 & d-1 & d \\ 0 & -(R+r) & d & d-1 \\ 1-d & -d & 0 & 0 \\ -d & 1-d & 0 & 0 \end{bmatrix} \begin{bmatrix} \hat{i}_{L1} \\ \hat{i}_{L2} \\ \hat{v}_{c1} \\ \hat{v}_{c2} \end{bmatrix} + \begin{bmatrix} 1 & (1-d)R \\ 0 & (1-d)R \\ 0 & d-1 \\ 0 & d-1 \end{bmatrix} \begin{bmatrix} V_{in} \\ I_{PN} \end{bmatrix} + \begin{bmatrix} V_{c1} + V_{c2} - I_{PN}R \\ V_{c1} + V_{c2} - I_{PN}R \\ -I_{L1} - I_{L2} + I_{PN}R \\ -I_{L1} - I_{L2} + I_{PN}R \end{bmatrix} \quad (1)$$

where the state variables are $\hat{x} = \begin{bmatrix} \hat{i}_{L1} & \hat{i}_{L2} & \hat{v}_{c1} & \hat{v}_{c2} \end{bmatrix}^T$, the input variables are $\hat{u} = \begin{bmatrix} \hat{V}_{in} & \hat{I}_{PN} \end{bmatrix}^T$, and $\hat{d}$.

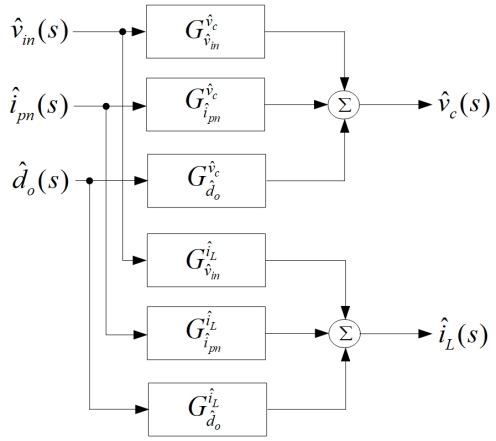

***Fig. 3**: Block diagram of qZSI plant model.*

To obtain the plant model of the considered system, the Laplace transform will be applied to (1) after that the block diagram of qZSI plant model is illustrated in Fig. 3. The plant equations of $G^{\hat{v}_c}_{\hat{v}_{in}}$, $G^{\hat{v}_c}_{\hat{i}_{pn}}$, $G^{\hat{v}_c}_{\hat{d}_0}$, $G^{\hat{i}_L}_{\hat{v}_{in}}$, $G^{\hat{i}_L}_{\hat{i}_{pn}}$, and $G^{\hat{i}_L}_{\hat{d}_0}$ in Fig. 3, can be calculated by Eqs. (2) - (7), respectively.

$$G^{\hat{v}_c}_{\hat{v}_{in}} = \frac{(1-D_0)(1-2D_0) - LCs^2(1-D_0)}{(LCs^2+1)(LCs^2+(1-2D_0)^2)} \tag{2}$$

$$G^{\hat{v}_c}_{\hat{i}_{pn}} = \frac{R(1-D_0)(1-2D_0) - (1-D_0)(Ls+r+R)}{LCs^2+C(r+R)s+(1-2D_0)^2} \tag{3}$$

$$G^{\hat{v}_c}_{\hat{d}_0} = \frac{(V_{c1}+V_{c2}-RI_{pn})(1-2D_0)}{LCs^2+C(r+R)s+(1-2D_0)^2} + \frac{(I_{pn}-I_{L1}-I_{L2})(Ls+r+R)}{LCs^2+C(r+R)s+(1-2D_0)^2} \tag{4}$$

$$G^{\hat{i}_L}_{\hat{v}_{in}} = \frac{[(LCs^2+D_0)+(1-D_0)(1-2D_0)]Cs}{LCs^2+(1-2D_0)^2} \tag{5}$$

$$G^{\hat{i}_L}_{\hat{i}_{pn}} = \frac{R(1-D_0)Cs+(1-D_0)(1-2D_0)}{LCs^2+C(r+R)s+(1-2D_0)^2} \tag{6}$$

$$G^{\hat{i}_L}_{\hat{d}_0} = \frac{(V_{c1}+V_{c2}-RI_{pn})Cs}{LCs^2+C(r+R)s+(1-2D_0)^2} + \frac{(I_{pn}-I_{L1}-I_{L2})(1-2D_0)}{LCs^2+C(r+R)s+(1-2D_0)^2} \tag{7}$$

From the plant model of qZSI, it can then be used to design the controller to operate in both shoot-through and non-shoot-through states. In addition, these equations can be also applied to optimize the considered system parameters in the future.

2.2 Control modes of qZSI

The considered system from Fig. 1 can be divided into standalone and grid-connected modes. The block diagram of qZSI control modes is shown in Fig. 4. For standalone mode as depicted in Fig. 4(a), it can be called "constant voltage control mode". The voltage across capacitor (v_{c1}) is regulated from the DC side using the PI controller when the breaker is off. In this mode, the inverter's output voltage at AC side will be also controlled by the remaining PI controller on d-q axes for the voltage amplitude and frequency regulations. Another mode is grid-connected mode that occurs when the breaker is on. The PI controller combined with MPPT algorithm will be applied, resulting in the MPP from PV rooftop feeding into the three-phase resistance load 20 Ω/phase and utility grid. For AC side control in the grid connection mode, PI controller will be used to control only the reference current because the voltage and frequency have been then synchronized. The controllers of DC and AC sides in both operation modes are designed by using the qZSI plant model as shown in Fig. 3. Many methods can be used to design these controllers such as phase lead or phase lag compensators, bode plot and root-locus methods [11]-[13].

***Table 1**: The PI controller parameters for the considered system.*

Parameter	Stand-alone mode	Grid connected mode
DC side control	$K_{i\_vcd} = 0.1$ $K_{p\_vcd} = 0.00468$	$K_{i\_vind} = -0.001$ $K_{p\_vind} = 0.0017$
AC side control	$K_{i\_vo} = 20$ $K_{p\_vo} = 0.005$ $K_{p\_ic} = 16$	$K_{i\_vcig} = -50$ $K_{p\_vcig} = -0.344$ $K_{i\_ig} = 300$ $K_{p\_ig} = 2.1$

For this paper, the root-locus method will be applied because it can provide a good steady-state error as well as time domain and transient responses. The deep details of the root-locus method for the controller design can be found in [14] and the parameters of PI controllers can be shown in Table 1. In addition, the parameter values of the proposed qZSI are set as follows: $L = 500\ \mu$H, $C = 400\ \mu$F, $R = 0.03\ \Omega$, $r = 0.47\ \Omega$, $I_{load} = 9.9$ A, $V_{in} = 130$ V, $M = 0.75$, $L_f = 4$ mH, $C_f = 450\ \mu$F, $R_f = 0.03\ \Omega$, $L_g = 10\ \mu$H, and $R_g = 0.2\ \Omega$.

3. FUZZY DESIGN FOR THE CONTROLLER OF QZSI

This section is the design of fuzzy logic controllers for qZSI operating in stand-alone mode and grid-connected mode. The fuzzy controller regulates the DC side system instead of the PI controller. The AC side controller of the considered system still uses a PI controller on the d-q axis. The control diagram for a quasi-source inverter connected with utility grid is shown in Fig. 5.

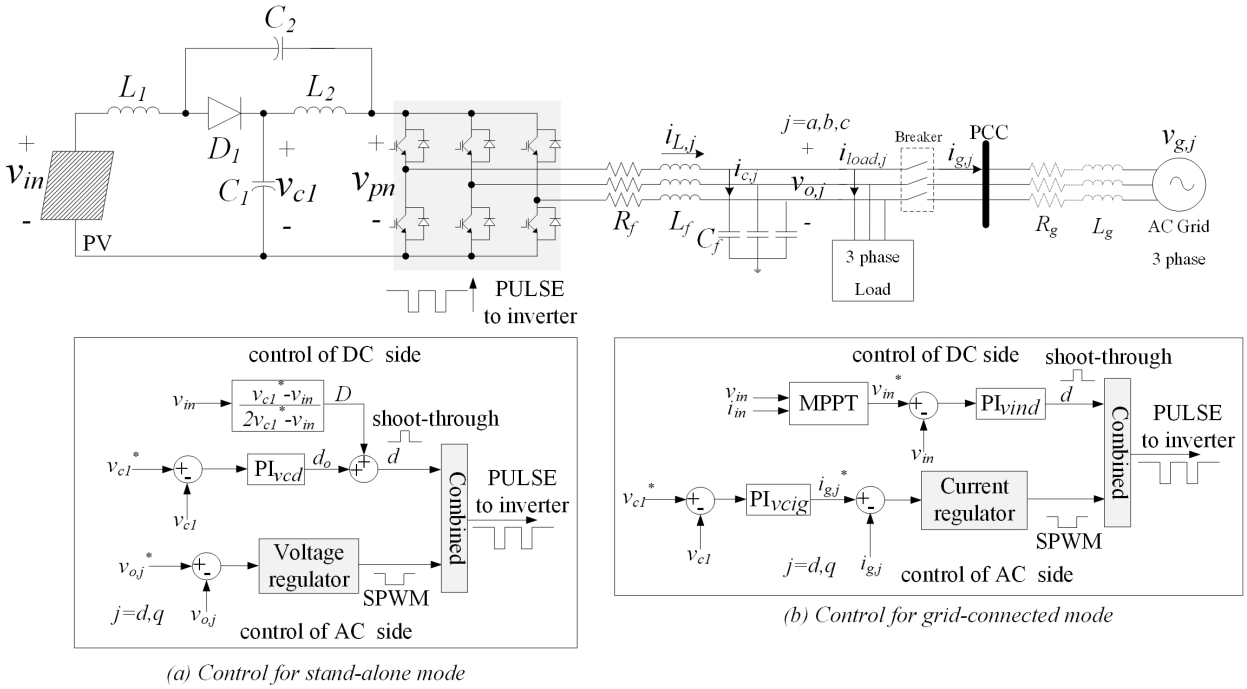

(a) Control for stand-alone mode

(b) Control for grid-connected mode

***Fig. 4**: Block diagram of control modes.*

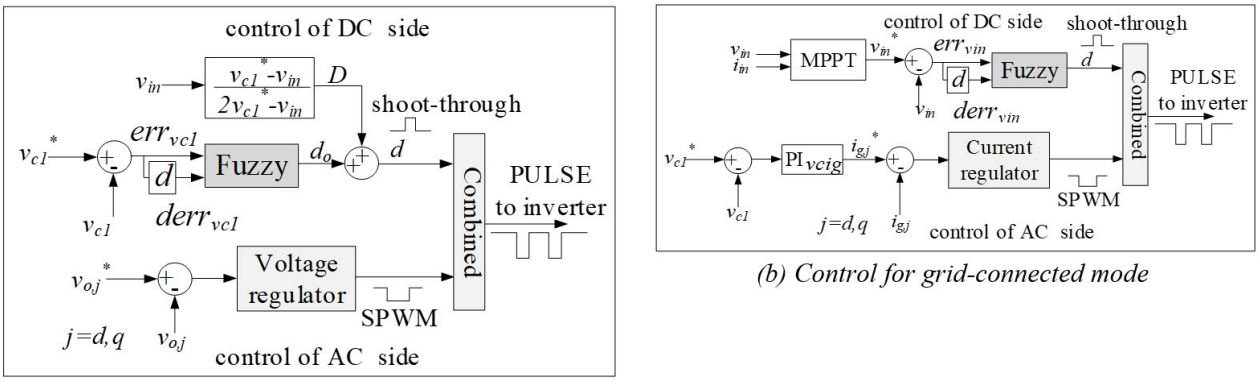

(a) Control for stand-alone mode

(b) Control for grid-connected mode

***Fig. 5**: Control diagram of a qZSI with fuzzy logic controller. (a) Control for stand-alone mode. (b) Control for grid-connected mode.*

3.1 Fuzzy Controller Design for stand-alone mode

In Fig. 5(a), the diagram shows the qZSI control structure for stand-alone mode. A fuzzy controller is used to control the voltage of the capacitor V_{c1}. The input value of controller is the error between $V_{c1}(err_{vc1})$ and the slope value of the V_{c1} error (err_rate_{vc1}). The output from the controller is the shoot-through duty rate (d_0).

The fuzzy controller design of qZSI for stand-alone mode uses triangular input membership function and straight-line tone output membership function as shown in Fig. 6(a) and 6(b), respectively.

The linguistic design of the error input member function determines three linguistic values: "neg", "zero", and "pos" as depicted in Fig. 6(a). The linguistic value of the error rate output member function is determined

***Table 2**: Fuzzy rules for regulating the voltage value accross capacitor (V_{c1}).*

error rate \ error	neg	zero	pos
neg_rate	dec	inc	inc
zero_rate	dec	cons	inc
pos_rate	dec	dec	inc

3 linguistic values. It consists of "neg_rate", "zero_rate", and "pos_rate" as implicitly shown in Fig. 6(b). Thus, the number of possible fuzzy rules for control is 9 (3x3=9). The fuzzy rules are shown in Table 2.

From the fuzzy rule in Table 2, when the input

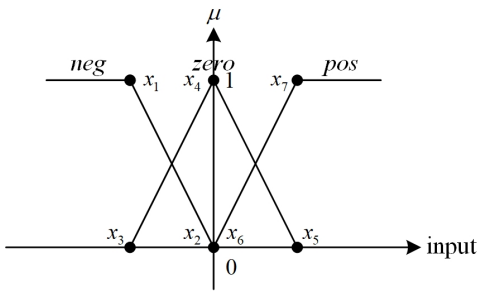

(a) Input membership function

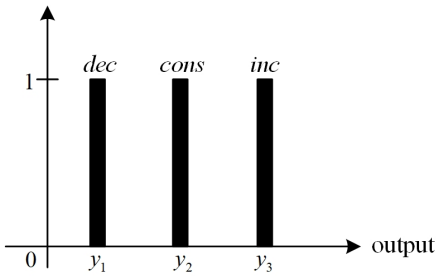

(b) Output membership function

***Fig. 6**: The membership function for the proposed fuzzy controller.*

***Table 3**: Fuzzy rules for regulating input voltage (V_{in}).*

error rate \ error	***neg***	***zero***	***pos***
neg_rate	*inc*	*dec*	*dec*
zero_rate	*inc*	*cons*	*dec*
pos_rate	*inc*	*inc*	*dec*

***Table 4**: Membership function for stand-alone mode.*

Input error member function position						
x_1	x_2	x_3	x_4	x_5	x_6	x_7
-5	0	-5	5	5	0	5
Input error rate member function position						
x_1	x_2	x_3	x_4	x_5	x_6	x_7
-2	0	-2	2	2	0	2
Output member function position						
y_1		y_2		y_3		
-0.2		0		0.2		

error value is negative and the input error rate is any value, the output value must be adjusted to reduce the shoot-through duty rate according to Rules 1-3. In addition, when the input error value is zero and the input error rate is positive, zero, or negative, the output value follows rule 4, 5, or 6, respectively.

In case of the input error value is positive and the input error rate is any value, the output value must be adjusted shoot-through duty rate incremented according to Rules 7-9. The fuzzy rules for controlling the voltage of a capacitor can be summarized as follows:

Rule 1 IF error = *neg* AND error rate = *neg_rate* THEN $d_0 = dec$

Rule 2 IF error = *neg* AND error rate = *zero_rate* THEN $d_0 = dec$

Rule 3 IF error = *neg* AND error rate = *pos_rate* THEN $d_0 = dec$

Rule 4 IF error = *zero* AND error rate = *neg_rate* THEN $d_0 = inc$

Rule 5 IF error = *zero* AND error rate = *zero_rate* THEN $d_0 = cons$

Rule 6 IF error = *zero* AND error rate = *pos_rate* THEN $d_0 = dec$

Rule 7 IF error = *pos* AND error rate = *neg_rate* THEN $d_0 = inc$

Rule 8 IF error = *pos* AND error rate = *zero_rate* THEN $d_0 = inc$

Rule 9 IF error = *pos* AND error rate = *pos_rate* THEN $d_0 = inc$

After the input of controller has been evaluated with fuzzy rules, the output is then calculated via the weighted average (WA) defuzzification method, a Takagi-Sugeno fuzzy inference [15]-[18]. This method is very simple for implementation. The positions of the input and output member functions can be determined by relationship of the considered system.

3.2 Fuzzy Controller Design for grid-connected mode

The control diagram for the grid-connected mode is depicted in Fig. 4(b). The input voltage (v_{in}) is controlled by a fuzzy controller in which it is the voltage at the maximum power point of the solar arrays using the MPPT algorithm. The input voltage error value (err_{vin}) and the difference of error values (err_rate_{vin}) are the fuzzy controller's inputs. The output of fuzzy controller is shoot-through duty (d). The grid-connected mode of a fuzzy logic controller for qZSI uses a triangular input member function and a straight-line tone output membership function. For this case, the linguistic design of the error rate input has 3 values and the linguistic value of the error rate input member function has also 3 linguistic values as well. As a result, there are 9 possible fuzzy rules (3x3=9) as shown in Table 3.

From the fuzzy rules for regulating the input voltage, the 9 rules are given in Table 3. When the input error value is negative and the input error rate is any value, the output d must be adjusted with shoot-through duty increments according to Rules 1-3. When the input error value is zero and the input error rate is negative, zero, or positive, the output value follows rule 4, 5, or 6, respectively. In addition, when the input error value is positive and the input error rate is any value, the output value must be reduced shoot-through duty according to rule 7-9. The fuzzy rules for controlling the input voltage

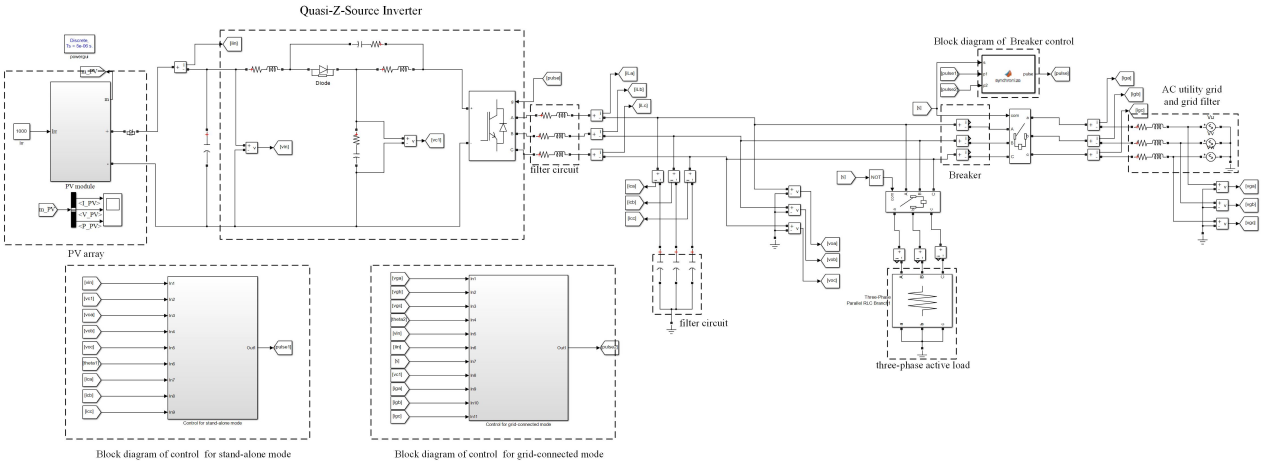

***Fig. 7**: Simulation model for the qZSI.*

***Table 5**: Membership function for grid-connected mode.*

Input error member function position						
x_1	x_2	x_3	x_4	x_5	x_6	x_7
-50	0	-50	50	50	0	50
Input error rate member function position						
x_1	x_2	x_3	x_4	x_5	x_6	x_7
-0.2	0	-0.2	0.2	0.2	0	0.2
Output member function position						
y_1		y_2		y_3		
0.18		0.2		0.22		

can be summarized as follows:

Rule 1 IF error = *neg* AND error rate = *neg_rate* THEN d = *inc*

Rule 2 IF error = *neg* AND error rate = *zero_rate* THEN d = *inc*

Rule 3 IF error = *neg* AND error rate = *pos_rate* THEN d = *inc*

Rule 4 IF error = *zero* AND error rate = *neg_rate* THEN d = *dec*

Rule 5 IF error = *zero* AND error rate = *zero_rate* THEN d = *cons*

Rule 6 IF error = *zero* AND error rate = *pos_rate* THEN d = *inc*

Rule 7 IF error = *pos* AND error rate = *neg_rate* THEN d = *dec*

Rule 8 IF error = *pos* AND error rate = *zero_rate* THEN d = *dec*

Rule 9 IF error = *pos* AND error rate = *pos_rate* THEN d = *dec*

The member function positions of the DC side fuzzy logic controllers for the qZSI in both stand-alone and grid-connected modes are shown in Table 4 and Table 5, respectively. The position of the membership function is obtained via trial-and-error method. The stand-alone mode input and output member function position shape is determined by the relationship between capacitor voltage and the shoot-through duty while the grid-connected mode is determined by the relationship between the voltage of the solar arrays and shoot-through duty.

4. SIMULATION RESULTS

According to Section 2, the locus-root approach was used to design the conventional PI controller for a qZSI, and the parameters of this controller are derived as indicated in Table 1. In addition, the fuzzy controller is designed for qZSI as provided in Section 3.

The SimPowerSystem® simulation was used to evaluate the control performance. The simulation determines that the system frequency of 50 Hz, the grid voltage 120 V_{rms} and the capacitor reference voltage $V_{c1}^{*} = 340$ V. The SimPowerSystem® model for both stand-alone and grid-connected modes are shown in Fig. 7.

The conditions for the simulation in both stand-alone and grid-connected modes were set by changing the irradiance from 1000 W/m^2 to 600 W/m^2, and 800 W/m^2 at 0.3 and 0.5 s, respectively.

For the stand-alone mode, the simulation results are given in Fig. 8. The voltage across capacitor is set equal to 340 V. The PI and the fuzzy controllers can regulate the capacitor voltage with the different irradiance. When the irradiance is varied suddenly, the transient response of the capacitor voltage demonstrates that the fuzzy controller can quickly reach into the command value. Moreover, the overshoot from the conventional PI controller is more than the proposed fuzzy controller. The results show that the fuzzy logic controller can provide better performance of the capacitor voltage of qZSI than the PI controller.

The simulation results of grid-connected mode are shown in Fig. 9. When the irradiance is changed, the voltage of the solar arrays (v_{in}) will be also changed equal to the voltage at the maximum power point of the solar arrays ($v_{in} = v_{mpp}$). The oscillation of p_{pv} is from the MPPT calculation. In this paper, the incremental conductance approach is used as the MPPT

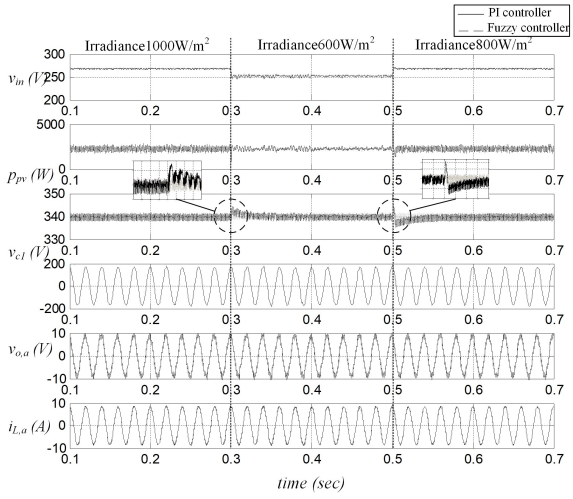

***Fig. 8**: Simulation results of stand-alone mode.*

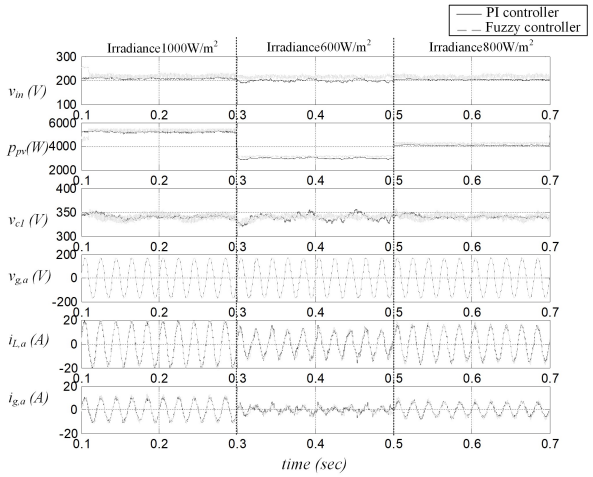

***Fig. 9**: Simulation results of grid-connected mode.*

algorithm. Fig. 10 shows the power response comparison at different irradiance between the fuzzy controller and the PI controller. The response of the system regulated by PI controller is the black line in which the grey line is the system response controlled by the Fuzzy logic. The responses shown that the fuzzy controller can perform the better power response, more efficient and fast response time than the PI controller. As a result, a higher power output of the solar arrays can be achieved.

Moreover, the $V_{c1} = 340\,\mathrm{V}$ and $V_{grid} = 120\,\mathrm{V}_{rms}$ corresponding to the reference voltage is defined. The current produced by the qZSI in grid-connected mode is higher than stand-alone mode because of the MPPT for solar arrays to achieve a higher power production. The load and grid are fed by the inverter current as shown in Fig. 9, which shows that the proposed controller can control a qZSI in grid-connected mode with a good performance.

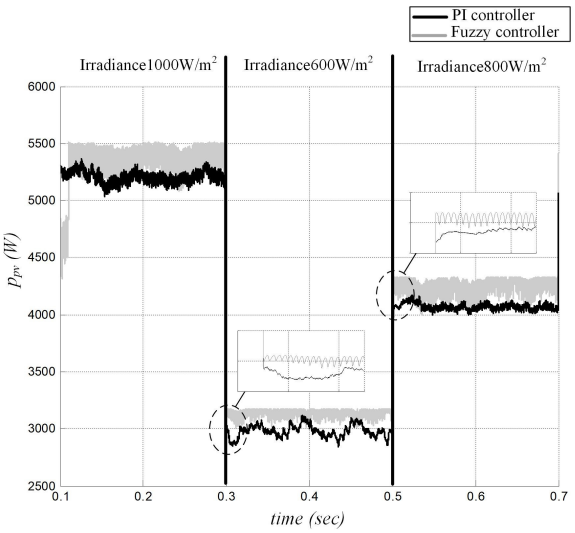

***Fig. 10**: The output power of the solar arrays of the qZSI in the grid-connected mode.*

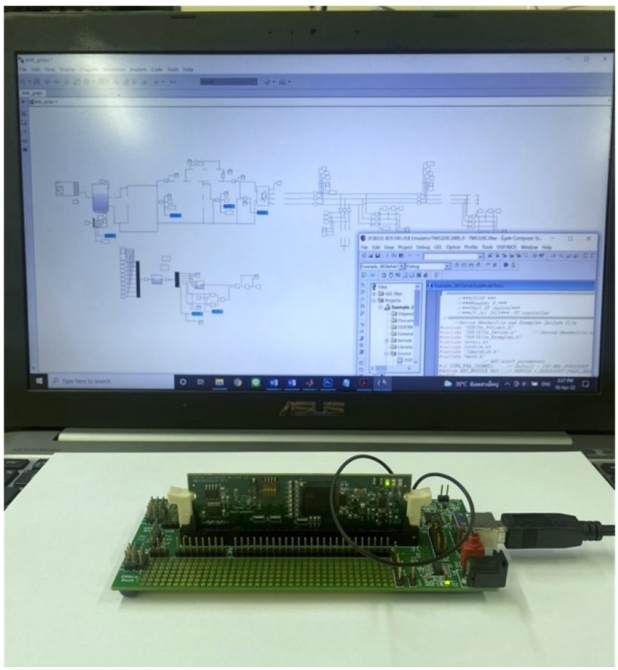

***Fig. 11**: HIL simulation connection.*

5. HIL SIMULATION RESULTS

Practically, the results simulated by SimPowerSystem® in MATLAB are not sufficient to confirm the performance of the proposed controller. To ensure that the proposed controller design for qZSI can be implemented in the microcontroller board, the hardware-in-loop (HIL) simulation will be used. In addition, HIL simulation can confirm that the system can operate by the proposed controller without the failure of practical conditions. In this paper, the eZdspTMF28335 was used to program the proposed controller in which this bord will be used to simulate along with the SimPowerSystem® in MATLAB. The connection between eZdspTMF28335 and

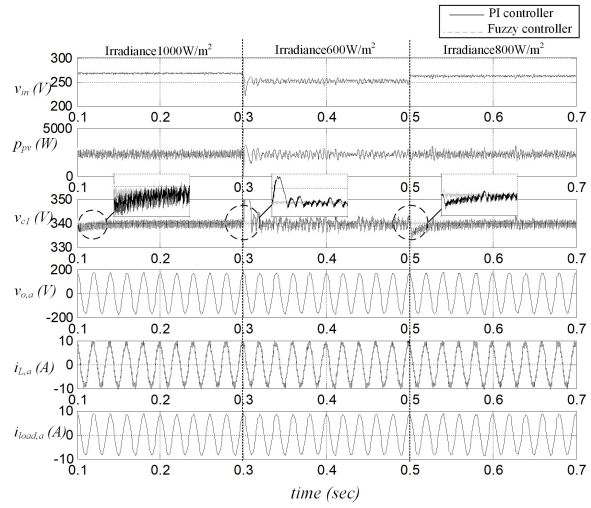

***Fig. 12**: HIL simulation results of stand-alone mode.*

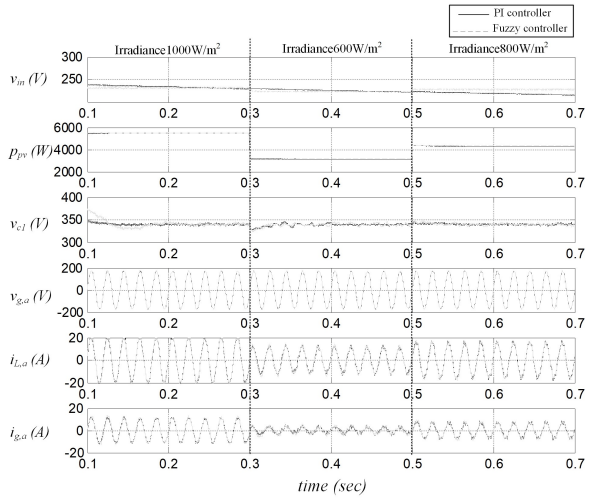

***Fig. 13**: HIL simulation results of grid-connected mode.*

the SimPowerSystem® in MATLAB can be depicted in Fig. 11.

From Fig. 11, both standalone and grid-connected modes of the considered system were used as the same connection between microcontroller board and MATLAB. In addition, the system parameters for HIL were set to the same as the simulation results. For the HIL simulation, the irradiance was changed from 1000 W/m^2 to 600 W/m^2, and 800 W/m^2 at the time instants 0.3 and 0.5 s, respectively. In this scenario, the reference voltage across the capacitor (V_{c1}^*) was set equal to 340 V and the reference output voltage of inverter ($v_{o,a}$) was defined at 120 V_{rms}. The results of standalone and grid-connected modes are illustrated in Fig. 12.

From Fig. 12, the V_{c1} can be regulated at 340 V in any irradiance by using the proposed controllers while the stand-alone mode is operated. For this mode, the fuzzy controller can provide the better performance in transient response compared with the PI controller at the time equal 0.3 and 0.5 s.

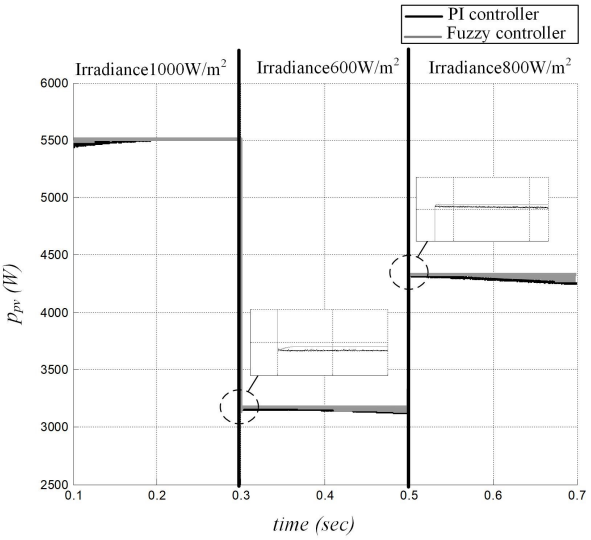

***Fig. 14**: Output power comparison of PV arrays grid-connected mode between PI and fuzzy controllers.*

In addition, the proposed controllers can be used to control the qZSI in the mode of grid-connection as depicted in Fig. 13. The V_{c1}^* can be controlled with the combination between the MPPT algorithm and the proposed controllers for tracking the MPP from PV arrays. In the grid-connection mode, the lower oscillation and faster response of V_{c1} can be achieved by the fuzzy controller. Moreover, when the output power from PV arrays (p_{pv}) is considered, the better response of p_{pv} can be also provided by the fuzzy controller as seen the zoom area of p_{pv} response in Fig. 14.

As for the HIL results in both mode operations, it can confirm that the fuzzy controller can provide the better performance compared with the conventional PI controller.

6. CONCLUSION

This paper presents a PV-Rooftop system operated in both stand-alone and grid-connected modes. The fuzzy logic controllers for the considered system used the triangular input membership function and the tone bar output membership function. There are 9 fuzzy rules for 3linguistic values. The membership function position of the fuzzy logic controller design was determined via trial-and-error approach. This is based on the relationship between the input voltage and shoot-through duty. The designed PI and fuzzy logic controllers were tested using simulation to verify the controller performance. According to simulation and HIL results, the proposed fuzzy controller can efficiently regulate the Quasi-Z-Source Inverter in both stand-alone and grid-connected modes compared with the conventional PI control.

ACKNOWLEDGMENTS

This work was supported by the research fund from Suranaree University of Technology, Thailand.

REFERENCES

[1] T. Meyer, "Photovoltaic Energy: Stand-Alone and Grid-Connected Systems," in *Encyclopedia of Energy*, C. J. Cleveland, Ed. New York: Elsevier, 2004, pp. 35-46.

[2] W. Chaichan, J. Waewsak, R. Nikhom, C. Kongruang, S. Chiwamongkhonkarn, and Y. Gagnon, "Optimization of stand-alone and grid-connected hybrid solar/wind/fuel cell power generation for green islands: Application to Koh Samui, southern Thailand," *Energy Reports*, vol. 8, pp. 480–493, Nov. 2022.

[3] J. Anderson and F. Z. Peng, "Four quasi-Z-Source inverters," *2008 IEEE Power Electronics Specialists Conference*, Jun. 2008.

[4] P. Fang Zheng, "Z-source inverter," *IEEE Transactions on Industry Applications*, vol. 39, no. 2, pp. 504–510, Mar. 2003.

[5] Y. Tang, J. Wei, and S. Xie, "A new direct peak dc-link voltage control strategy of Z-source inverters," *2010 Twenty-Fifth Annual IEEE Applied Power Electronics Conference and Exposition (APEC)*, Palm Springs, CA, USA, 2010, pp. 867-872.

[6] Y. Liu, *Impedance source power electronic converters*, First edition ed. Chichester, West Sussex, United Kingdom: John Wiley and Sons, Inc, 2016, p. 1.

[7] P. C. Loh, D. M. Vilathgamuwa, C. J. Gajanayake, Y. R. Lim, and C. W. Teo, "Transient Modeling and Analysis of Pulse-Width Modulated Z-Source Inverter," *IEEE Transactions on Power Electronics*, vol. 22, no. 2, pp. 498–507, Mar. 2007.

[8] W. Mo, P. C. Loh and F. Blaabjerg, "Model predictive control for Z-source power converter," *8th International Conference on Power Electronics - ECCE Asia*, Jeju, Korea (South), 2011, pp. 3022-3028.

[9] Y. Li, S. Jiang, J. G. Cintron-Rivera, and F. Z. Peng, "Modeling and Control of Quasi-Z-Source Inverter for Distributed Generation Applications," *IEEE Transactions on Industrial Electronics*, vol. 60, no. 4, pp. 1532–1541, Apr. 2013.

[10] M. K. Kazimierczuk, "Small-Signal Modeling of Open-Loop PWM Z-Source Converter by Circuit-Averaging Technique," *IEEE Transactions on Power Electronics*, vol. 28, no. 3, pp. 1286–1296, Mar. 2013.

[11] J. Liu, J. Hu, and L. Xu, "Dynamic Modeling and Analysis of Z Source Converter—Derivation of AC Small Signal Model and Design-Oriented Analysis," *IEEE Transactions on Power Electronics*, vol. 22, no. 5, pp. 1786–1796, Sep. 2007.

[12] C. H. van der Broeck, R. W. De Doncker, S. A. Richter, and J. von Bloh, "Unified Control of a Buck Converter for Wide-Load-Range Applications," *IEEE Transactions on Industry Applications*, vol. 51, no. 5, pp. 4061–4071, Sep. 2015.

[13] Y. Li, F. Z. Peng, J. G. Cintron-Rivera and S. Jiang, "Controller design for quasi-Z-source inverter in photovoltaic systems," *2010 IEEE Energy Conversion Congress and Exposition*, Atlanta, GA, USA, 2010, pp. 3187-3194.

[14] P. Wongyai, K. Areerak and K. Areerak, "PI Controller Design Using root-locus For Quasi-Z-Source Inverter," *2019 16th International Conference on Electrical Engineering/Electronics, Computer, Telecommunications and Information Technology (ECTI-CON)*, Pattaya, Thailand, 2019, pp. 549-552.

[15] E. H. Mamdani, "Application of Fuzzy Algorithms for Control of Simple Dynamic Plant," *Proceedings of the IEEE*, Vol. 121, No. 12, 1974, pp. 1585-1588..

[16] R. M. Hilloowala and A. M. Sharaf, "A rule-based fuzzy logic controller for a PWM inverter in photo-voltaic energy conversion scheme," *Conference Record of the 1992 IEEE Industry Applications Society Annual Meeting*, Houston, TX, USA, 1992, pp. 762-769 vol.1.

[17] B. Hamed and N. A. Qaoud, "Fuzzy Control Design for Quasi-Z-Source Three Phase Inverter," *2019 IEEE 7th Palestinian International Conference on Electrical and Computer Engineering (PICECE)*, Gaza, Palestine, 2019, pp. 1-6.

[18] R. Ramya and T. S. Sivakumaran, "Design And Control Strategies of Quasi – Z Source Inverter For Photovoltaic Power Generation Systems," *2020 5th International Conference on Devices, Circuits and Systems (ICDCS)*, Coimbatore, India, 2020, pp. 262-266.

Patumporn Wongyai was born in Lamphun, Thailand, in 1991. She received the B.Eng. (first-class honors) and M.Eng. degrees in electrical engineering from Suranaree University of Technology (SUT), Nakhon Ratchasima, Thailand, in 2014 and 2016 respectively. Now, she study in Ph.D. of electrical engineering in SUT. Her main research interests include power electronics, modeling of power electronic system, solar energy conversion and control theory.

Jakkrit Pakdeeto received B.Eng. (first-class honors), M.Eng., and Ph.D. degrees in electrical engineering from Suranaree University of Technology (SUT), Nakhon Ratchasima, Thailand, in 2013, 2015 and 2019, respectively. In 2019, he was a researcher in Institute of research and development at SUT. Since 2020, he has been a lecturer in the department of Teacher Training in Electrical Engineering, Faculty of Technical Education, King Mongkut's University of Technology (KMUTNB), Thailand. He has received the Assistant Professor in Electrical Engineering in 2021. His main research interests include stability analysis, power electronics, AI applications, control theory and DC micro-grid systems.

Koson Chaicharoenaudomrung received B.Eng, M.Eng, and Ph.D. degrees in electrical engineering from Suranaree University of Technology (SUT), Nakhon Ratchasima, Thailand, in 2008 2011 and 2018, respectively. In 2019, he was a researcher in research and development at SUT. Since 2020, he has been a lecturer in the Department of Electrical Engineering Technology, College of Industrial Technology, King Mongkut's University of Technology North Bangkok (KMUTNB), Thailand. He has received the Assistant Professor in Electrical Engineering in 2022. His main research interests include stability analysis, modeling of power electronic system, wind energy conversion system, power electronic and control system, and AI application.

Kongpol Areerak received the B.Eng, M.Eng, and Ph.D. degrees in electrical engineering from Suranaree University of Technology (SUT), Thailand, in 2000, 2003, and 2007, respectively. Since 2007, he has been a lecturer and Head of Power Quality Research Unit (PQRU) in the School of Electrical Engineering, SUT. He received the Associate Professor in Electrical Engineering in 2015. His main research interests include active power filter, harmonic elimination, AI application, motor drive, and intelligence control systems.

Kongpan Areerak received the B.Eng. M.Eng degrees from Suranaree University of Technology (SUT), Nakhon Ratchasima, Thailand, in 2000 and 2001, respectively and the Ph.D. degree from the University of Nottingham, Nottingham, UK., in 2009, all in electrical engineering. In 2002, he was a lecturer in the Electrical and Electronic Department, Rangsit University, Thailand. Since 2003, he has been a Lecturer in the School of Electrical Engineering, SUT. He has received the Associate Professor in Electrical Engineering in 2015. His main research interests include system identifications, artificial intelligence applications, stability analysis of power systems with constant power loads, modeling and control of power electronic based systems, and control theory.